1

Acid–Base Cooperative Catalysis for Organic Reactions by Designed Solid Surfaces with Organofunctional Groups

Ken Motokura, Toshihide Baba, and Yasuhiro Iwasawa

1.1

Introduction

This chapter deals with acid–base bifunctional heterogeneous catalyst surfaces with organofunctional groups. One of the most important issues for bifunctional heterogeneous catalysis is the coexistence of incompatible catalytic species, such as acid and base, nearby on a same solid particle surface. In nucleophilic reactions, acid–base bifunctional catalysts enable the activation of both nucleophilic and electrophilic substrates to enhance their reactions. Generally, there are two types of catalytic nucleophilic addition reactions: the first one is activation of the nucleophile precursors by basic catalysts to abstract their acidic parts, such as α-hydrogen atoms, and the other is the lowering of lowest unoccupied molecular orbital (LUMO) levels of electrophiles by interaction with Brønsted or Lewis acidic catalysts. From this fact, an ideal pathway for the nucleophilic reaction is dual activation of both electrophiles and nucleophiles by acidic and basic functions of catalysts, respectively (Scheme 1.1) [1]. Strongly acidic and basic species in a solution reactor induces neutralization immediately, thus affording inactive salts. However, immobilization of both the acidic and basic species on solid surfaces can avoid mutual neutralization. Some catalytic reaction systems containing both acidic and basic solid catalysts as separate catalyst particles have been reported for one-pot reaction sequences [2]. In these reaction systems, the acid and base sites are immobilized on different catalyst particles. Therefore, it is difficult to accelerate a single reaction step by cooperative activation of two substrates by both acid and base sites.

Immobilization of acidic and basic species nearby on a same solid surface can create a bifunctional catalytic surface possessing acid and base species that are able to participate in a single reaction step, resulting in significant acceleration of the catalytic reaction. Several reviews have been published on such heterogeneous acid–base catalysts having organic functional groups [3]. These heterogeneous acid–base bifunctional catalysts can be categorized into the following two types: (i) catalysts possessing both immobilized acidic and basic organic groups on their surfaces and (ii) catalysts possessing immobilized basic organic groups and acid sites derived from their support surfaces. In this chapter, these two types of

Bridging Heterogeneous and Homogeneous Catalysis: Concepts, Strategies, and Applications, First Edition.
Edited by Can Li and Yan Liu.

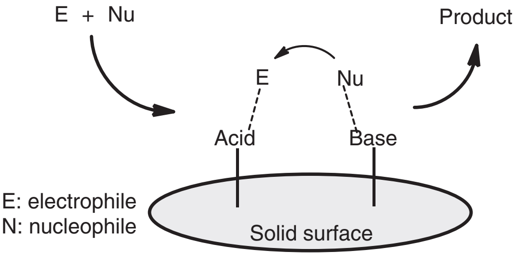

Scheme 1.1 Dual activation of both electrophile (E) and nucleophile (Nu) by acid and base sites on a solid surface.

acid–base bifunctional catalysts are introduced and their catalytic performances are discussed.

1.2
Bifunctional Catalysts Possessing Both Acidic and Basic Organic Groups

1.2.1
Urea–Amine Bifunctional Catalyst

In 2005, Lin and coworkers [4] demonstrated urea–amine bifunctionalized silica surfaces for C–C couplings, such as aldol reaction of acetone, nitroaldol reaction (Henry reaction), and cyanosilylation. Surface structures of these immobilized mesoporous silica nanospheres (MSNs) are shown in Figure 1.1. Both urea (UDP, ureidopropyl group) and amine (AEP, 3-(2-(2-aminoethylamino)ethylamino)propyl group)-immobilized mesoporous silica nanosphere (AEP/UDP-MSN) showed the highest catalytic activity among amine- or urea-immobilized MSNs (AEP- or UDP-MSN) (Scheme 1.2). In addition, these reactions were not significantly enhanced by a physical mixture of AEP-MSN and UDP-MSN. Scheme 1.3 represents a proposed reaction pathway of the aldol reaction involving activation of the aldehyde and acetone by urea (acid) and amine (base) group, respectively, on the silica surface.

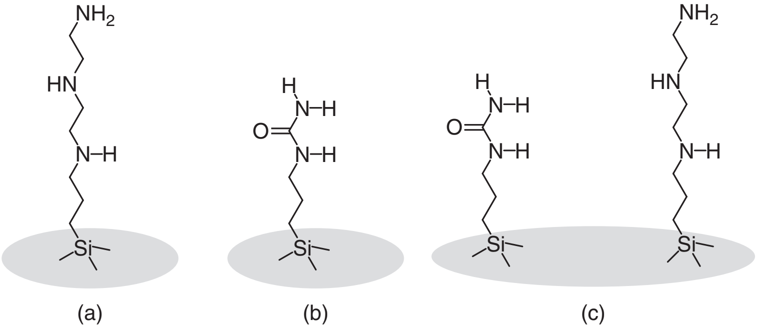
(a) (b) (c)

Figure 1.1 Surface structures of (a) AEP-, (b) UDP-, and (c) AEP/UDP-immobilized mesoporous silica nanosphere (MSN).

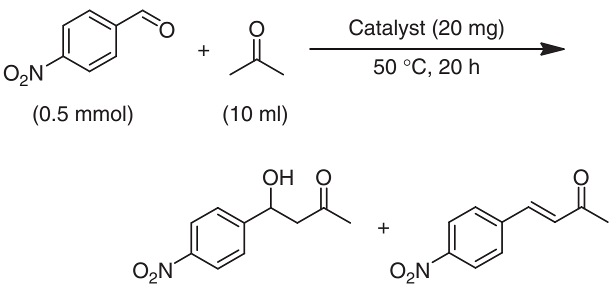

Catalyst	TON
AEP/UDP-MSN	22.6
AEP-MSN	5.4
UDP-MSN	0.0
AEP-MSN + UDP-MSN (20 mg + 20 mg)	6.4

Scheme 1.2 Aldol reaction of acetone with 4-nitrobenzaldehyde using urea and amine groups-immobilized mesoporous silica nanospheres.

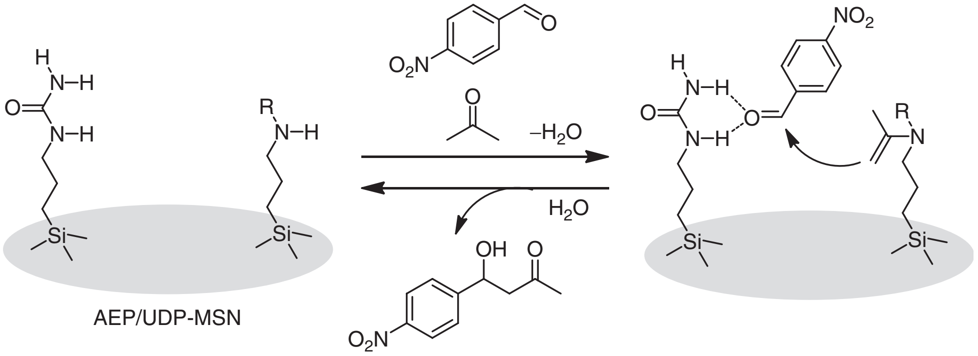

Scheme 1.3 Proposed reaction pathway of aldol reaction using urea and amine groups-immobilized mesoporous silica nanosphere (AEP/UDP-MSN).

1.2.2
Sulfonic or Carboxylic Acid–Amine Bifunctional Catalyst

The first report on the immobilization of incompatible organic acid and base groups on a same catalyst particle surface was given by Davis and coworkers in 2006 [5]. They reported SBA-15 containing both benzene sulfonic acid (A) and primary amine (B) groups (SBA-15-AB). The structure of SBA-15-AB is shown in Figure 1.2. Table 1.1 presents the catalytic performances for aldol reaction of acetone and 4-nitrobenzaldehyde. SBA-15-AB showed 62% conversion of aldehyde,

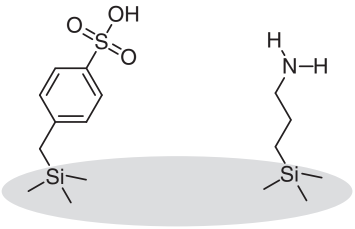

SBA-15-A/B

Figure 1.2 Surface structure of SAB-15-containing sulfonic acid and primary amine groups (SBA-15-AB).

Table 1.1 Aldol reactions using heterogeneous and homogeneous acid and base catalysts.[a]

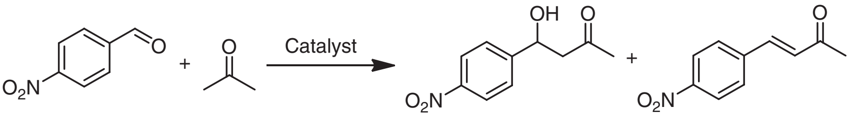

Entry	Catalyst	Conversion of aldehyde (%)
1	SBA-15-A/B	62
2	SBA-15-A	16
3	SBA-15-B	33
4	SBA-15-A + SBA-15-B	44
5	SBA-15	0
6	*p*-Toluenesulfonic acid + *n*-propylamine	0
7	*p*-Toluenesulfonic acid	4
8	*n*-Propylamine	8
9	SBA-15-A/B + *p*-toluenesulfonic acid	14
10	SBA-15-A/B + *n*-propylamine	38

[a] Catalyst (sulfonic acid: 0.05 mmol, amine: 0.05 mmol), 4-nitrobenzaldehyde (0.5 mmol), acetone (10 ml), Ar, 50 °C, 20 h.

while SAB-15 supported only sulfonic acid (SBA-15-A) or the primary amine (SBA-15-B) showed 16% and 33% conversion, respectively, of the aldehyde. This result demonstrates the cooperative catalysis of the sulfonic acid and primary amine groups immobilized on the same SBA-15 surface. The physical mixture of SAB-15-A and SAB-15-B showed 44% conversion, indicating that the acidic and basic materials on separate supports did not show the cooperative activity efficiently. The addition of a homogeneous acid, *p*-toluenesulfonic acid, to the SAB-15-AB catalyst induced a significant decrease of its catalytic activity. The addition of homogeneous amine also showed a similar phenomenon. Zeidan and Davis [5b] also reported an acid–base bifunctional catalyst having phosphoric or carboxylic acid – weaker acids than sulfonic acid – as the organic acid group. The carboxylic acid/amine-functionalized silica showed the highest catalytic activity as a result of the increased number of free acid/base groups.

After the reports of Davis and coworkers [5], several bifunctional catalysts with both organic acid and base groups have been reported and used for carbon–carbon bond-forming reactions [6]. Thiel and coworkers [6a] reported sulfonic acid/amine-functionalized mesoporous silica nanoparticles (MSN) for nitroaldol reaction of nitromethane with 4-hydroxybenzaldehyde. They prepared primary amine-, diamine-, benzene sulfonic acid-functionalized MSNs, denoted as MSN-NH_2, MSN-NNH_2, and MSN-SO_3H, respectively. Both amines and sulfonic acid-functionalized MSN were also prepared (MSN-NH_2-SO_3H and MSN-NNH_2-SO_3H). The catalytic performances are summarized in Table 1.2. MSN-NNH_2 (entry 2) showed a higher activity than MSN-NH_2 (entry 1). While MSN-SO_3H did not show any catalytic activity (entry 3), MSN-NH_2-SO_3H (entry 4), and MSN-NNH_2-SO_3H (entry 5) showed higher performances than those of the only amine-functionalized MSNs. In the case of a physical mixture of acid- and base-functionalized MSN (MSN-NNH_2 + MSN-SO_3H) (entry 6), the product yield was significantly lower than that obtained by MSN-NNH_2-SO_3H (entry 5). These results suggest that the immobilized acid and base groups on the same silica particle surface realizes a cooperative catalytic enhancement. However, it is to be noted that no catalytic activity was observed after removal of surface silanol (Si-OH) groups from MSN-NNH_2-SO_3H

Table 1.2 Nitroaldol reactions using amine- and sulfonic acid-functionalized MSN.[a]

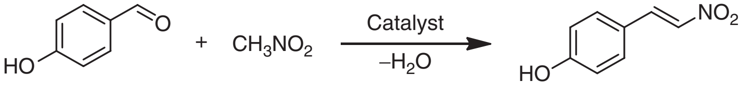

Entry	Catalyst	*t* (h)	Yield (%)
1	MSN-NH_2	6	33
2	MSN-NNH_2	6	44
3	MSN-SO_3H	12	0
4	MSN-NH_2-SO_3H	6	60
5	MSN-NNH_2-SO_3H	6	96
6[b]	MSN-NNH_2 + MSN-SO_3H	6	54
7[c]	Sil-MSN-NNH_2-SO_3H	6	0
8	MSN-NNH_2-Cl	6	71
9[d]	MSN	12	0

[a] 4-Hydroxybenzaldehyde (1 mmol), nitromethane (10 ml), catalyst (amine: 0.025 mmol), N_2 atmosphere, 90 °C.

[b] 1 : 1 physical mixture of acid and base.

[c] Silylated sample.

[d] Fifty milligrams of MSN was used.

by capping reaction using phenyltrimethoxysilane (Sil-MSN-NNH_2-SO_3H, entry 7). This result indicates that the surface silanol groups are necessary for the cooperative catalysis between the sulfonic acid and amine groups. The catalytic activity decreased by replacement of the sulfonic acid group in MSN-NNH_2-SO_3H by the chloropropyl function (MSN-NNH_2-Cl, entry 8). Overall, the sulfonic acid group alone cannot enhance the reaction, but sulfonic acid enhances the catalytic reaction in the presence of both amine and silanol groups.

In contrast to the above report for the carboxylic acid/amine-functionalized silica by Zeidan and Davis [5b], in 2012 Jones and coworkers [7] demonstrated a negative impact of the introduction of carboxylic acid group to the primary amine-functionalized silica for aldol reaction. SBA-15 was used as a mesoporous silica support. The surface structures of functionalized SBA-15 reported in the literature are shown in Figure 1.3. For example, the aminopropyl group (AP)-grafted SBA-15 with 0.5 mmol g^{-1} of theoretical loading is denoted as SBA-G-AP0.5. Aldol reaction of acetone with 4-nitrobenzaldehyde, which is the same reaction as that used in the previously reported carboxylic acid/amine-functionalized silica [5b], was chosen as a test reaction. Table 1.3 represents initial turnover frequency (TOF) values of the aldol reaction using various catalysts. Among the catalysts employed, the primary amine-grafted SBA-15 (SBA-G-AP0.5) showed the highest catalytic activity (entry 1). Introduction of carboxylic acid protected as ester (SBA-G-AP0.5-E0.5) induced a decrease in the catalytic activity (entry 2). The initial TOF values further decreased after the deprotection of the ester to form the carboxylic acid

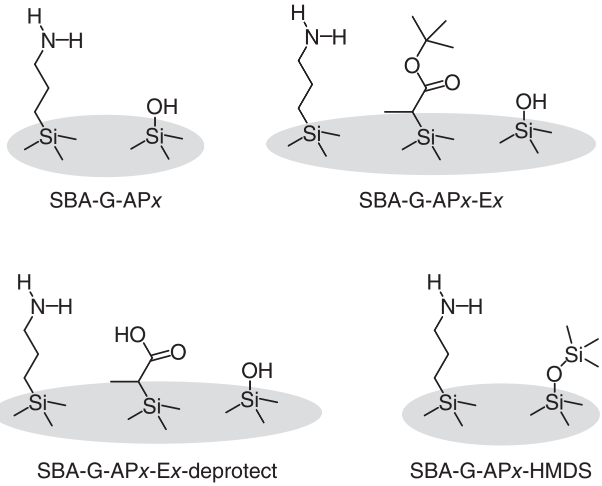

Figure 1.3 Surface structures of amine and/or carboxylic acid grafted silica catalysts. The organosilanes used for functionalization were aminopropyltrimethoxysilane (AP) and *t*-butyl 2-methyl-3-(triethoxysilyl)propanoate (E). The amount of theoretical loading is denoted as "*x*." Thus, a material prepared through grafting AP (0.5 mmol g^{-1}), followed by E (0.5 mmol g^{-1}) would be labeled SBA-G-AP0.5-E0.5.

Table 1.3 Initial TOF for the different catalysts in aldol reactions.[a]

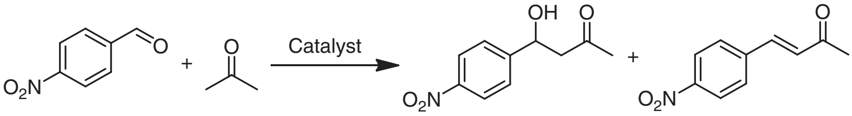

Entry	Catalyst	Initial TOF (h^{-1})
1	SBA-G-AP0.5	2.6
2	SBA-G-AP0.5-E0.5	1.5
3	SBA-G-AP0.5-E0.5-deprotect	1.2
4	SBA-G-AP0.5-E4.0	0.3
5	SBA-G-AP0.5-HMDS	0.8

[a] Catalyst (amine: 0.025 mmol), 4-nitrobenzaldehyde (0.25 mmol), acetone (5 ml), N_2, 50 °C.

group (SBA-G-AP0.5-E0.5-deprotect, entry 3). Increasing the amount of carboxylic acid protected as ester (SBA-G-AP0.5-E4.0, entry 4) or removal of silanols by the treatment with hexamethyldisiloxane (HMDS) (SBA-G-AP0.5-HMDS, entry 5) decreased the catalytic activity. The authors conjunctured that the second organic group presumably occupied silanol groups adjacent to the amine sites, inhibiting the cooperative catalysis between amines and silanols.

The above report by Jones and coworkers strongly indicates that it is necessary to keep the amount of silanols constant for the investigation of the cooperative catalysis of both organic acid and base groups. Additionally, it can be said that surface silanol groups possess potential usefulness for the promotion of amine-catalyzed reactions. The detailed role of silanol groups in the cooperative catalysis will be discussed in the next section.

1.3
Bifunctional Catalysts Possessing Basic Organic Groups and Acid Sites Derived from Their Support Surface

1.3.1
Organic Base-Catalyzed Reactions Enhanced by SiO_2

Amine-catalyzed aldol reaction enhanced by SiO_2 was reported by Kubota and coworkers in 2003 [8]. In the reaction of 4-nitrobenzaldehyde with acetone catalyzed by piperazine, the addition of mesoporous silica FSM-16 induced the increase in yield of the product from 5% to 91%. Several secondary amines were used as catalysts. In addition, the authors also investigated the amine-immobilized silicas

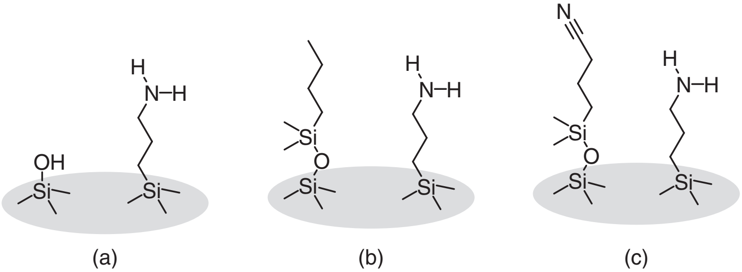

Figure 1.4 Amine-functionalized silicas: (a) silica possessing both primary amine and silanol group (polar/acidic), (b) primary amine and alkyl group (nonpolar/nonacidic), and (c) primary amine and nitrile function (polar/nonacidic).

as catalysts for the aldol reaction. The authors expected that the silanols on the silicate wall could be assisting the increase in catalytic activity.

In 2006, Katz and coworkers [9] investigated the detailed acid–base bifunctional catalysis of an immobilized primary amine on silica and silanol groups on the same silica surface. They prepared three types of amine-functionalized silicas (Figure 1.4): (i) silica possessing both primary amine and silanol groups (polar/acidic), (ii) primary amine and alkyl groups (nonpolar/nonacidic), and (iii) primary amine and nitrile groups (polar/nonacidic). Knoevenagel condensation, nitroaldol reaction, and Michael reaction were examined as catalytic reactions using these silica-supported primary amines. Based on the highest activity of the polar/acidic silica for the Knoevenagel reaction of malononitrile with 3-nitrobenzaldehyde (Table 1.4), the authors demonstrated the imine catalytic mechanism involving activation of an aldehyde (electrophile) and an imine intermediate by the surface silanol groups (Scheme 1.4).

Table 1.4 Aldol reactions using heterogeneous and homogeneous acid and base catalysts.[a]

Entry	Catalyst	k_{app} (h^{-1})
1	Polar/acidic	2.9
2	Nonpolar/nonacidic	0.22
3	Polar/nonacidic	0.48

[a] $-dC_{aldehyde}/dt = k_{app}\ C_{aldehyde}$: at low conversion of reaction. In the reaction of nonacidic catalyst, mesoporous silica (an equivalent number of silanol) was added. The amount of catalyst was fixed at 0.01 M equiv of amine relative to 3-nitrobenzaldehyde. Eight milliliters of benzene solution of concentration 0.022 M in 3-nitrobenzaldehyde and 0.044 M of malononitrile was used.

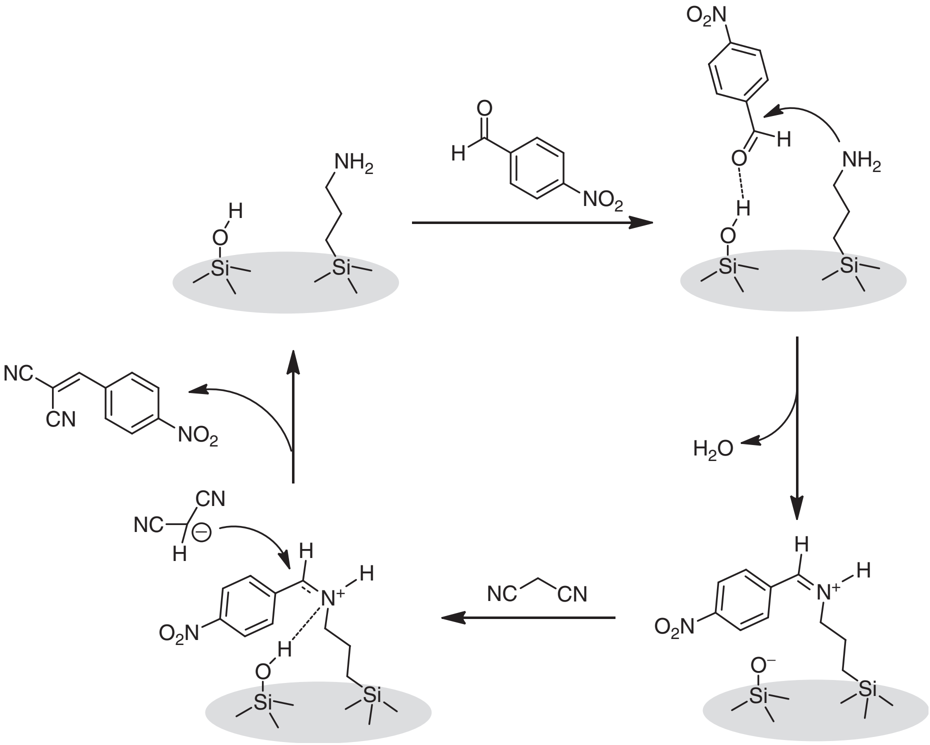

Scheme 1.4 Reaction pathway of Knoevenagel reaction using silica-supported primary amine (polar/acidic) catalyst.

Sharma and Asefa [10] demonstrated primary amine-functionalized MCM-41 for the nitroaldol reaction. Amine-functionalized MCM-41 catalysts were synthesized by the post-grafting method using ethanol solvent at 78 °C (AP-E1; AP group) and toluene at 78 °C (AP-T1) and under reflux (AP-T2). The loading amounts of amine groups in these materials were 1.3 (AP-E1), 4.1 (AP-T1), and 4.3 $\mathrm{mmol\,g^{-1}}$ (AP-T2). The catalytic reaction results of nitroaldol reactions of nitromethane with 4-hydroxybenzaldehyde are summarized in Scheme 1.5. The authors mentioned the following two reasons for the highest performance of AP-E1: (i) the higher number of silanol groups in AP-E1 activating the carbonyl group of benzaldehyde (as shown in Scheme 1.4) and (ii) the higher surface area of AP-E1 due to its lower density of grafted organoamines.

The above studies [8–10] strongly indicate the participation of silanol groups as acid sites in the amine-catalyzed reactions. The synergistic catalysis of immobilized organic bases and silanol groups has been highlighted by the cyclic carbonate synthesis from carbon dioxide and epoxide. Acid–base dual activation mechanism of the cyclic carbonate synthesis is widely accepted. Sakakura and coworkers [11] reported silica-supported phosphonium salts as highly active catalysts for the cyclic carbonate synthesis. The results for propylene carbonate synthesis are summarized

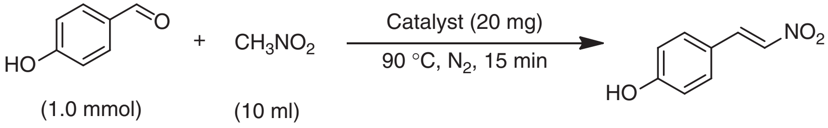

Catalyst	Conversion (%)
AP-E1	99.0
AP-T1	52.5
AP-T2	3.2
MCM-41	0.0

Scheme 1.5 Nitroaldol reaction using amine-functionalized MCM-41 prepared in ethanol at 78 °C (AP-E1) and in toluene at 78 °C (AP-T1) and under reflux (AP-T2).

Table 1.5 Cyclic carbonate synthesis from CO_2 and propylene oxide.[a]

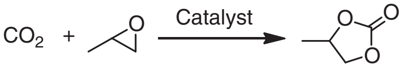

Entry	Catalyst	Yield (%)	k (min^{-1})
1	$P(n\text{-}Bu)_4Br$	4	0.07
2	$P(n\text{-}Bu)_4I$	5	0.09
3	$SiO_2\text{-}C_3H_6\text{-}P(n\text{-}Bu)_4Br$	53	4.1
4	$SiO_2\text{-}C_3H_6\text{-}P(n\text{-}Bu)_4I$	100	26
5	$SiO_2\text{-}(4\text{-}C_6H_4)CH_2\text{-}P(n\text{-}Bu)_4Br$	37	2.5
6	$PS\text{-}(4\text{-}C_6H_4)CH_2\text{-}P(n\text{-}Bu)_4Br$	9	0.22

[a] CO_2 (10 MP), propylene oxide (57.2 mmol), 100 °C, 1 h, catalyst (halogen: 0.57 mmol).

in Table 1.5. Silica-supported phosphonium salts [$SiO_2\text{-}C_3H_6\text{-}P(n\text{-}Bu)_4X$] showed much higher catalytic performance compared to homogeneous phosphonium salts [$P(n\text{-}Bu)_4X$] (entries 3 and 4 vs entries 1 and 2). The phosphonium group bound to the silica surface by a rigid 4-phenylenemethylene-linker [$\text{-}(4\text{-}C_6H_4)CH_2\text{-}$] showed a much lower performance (entry 5). Replacement of SiO_2 support with polystyrene (PS) decreased significantly the catalytic activity (entry 6). These results indicate that the reaction was promoted by the cooperative catalysis by the phosphonium salt part and silica surface. The proposed reaction pathway involving the cooperative activation by the anion part of the onium salts (X^-) and silanols is shown in Scheme 1.6. We also reported cyclic carbonate synthesis using a silica-supported aminopyridinium halide catalyst [12]. The reaction of propylene oxide proceeded under 1 atm of CO_2 at 30 °C, as shown in Scheme 1.7.

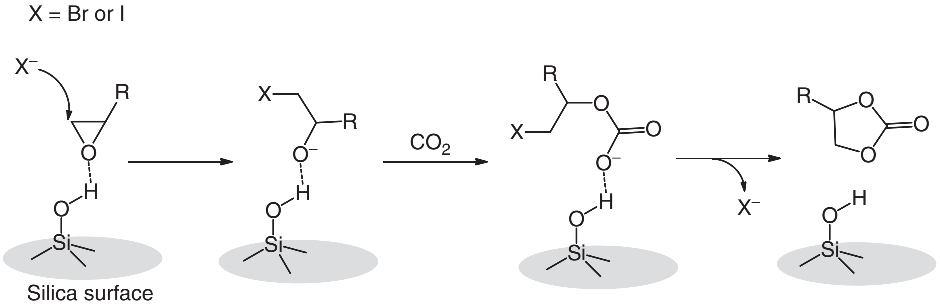

Scheme 1.6 Proposed reaction pathway of the silica-supported phosphonium halide-catalyzed cyclic carbonate synthesis from CO_2 and epoxide.

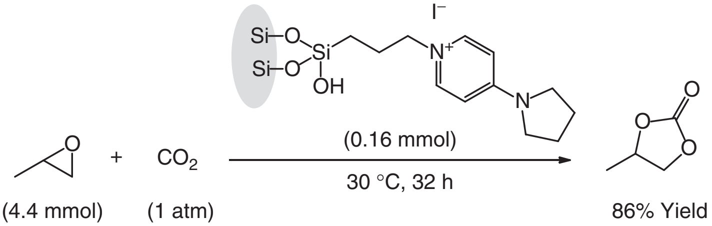

Scheme 1.7 SiO_2-supported aminopyridinium iodide-catalyzed propylene carbonate synthesis under 1 atm of CO_2.

1.3.2
Amine-Catalyzed Reactions Enhanced by Acid Site on Silica–Alumina

Owing to the weak acidity of the silanol groups, the coexistence of organic amines and silanols is very easy. However, their restricted application to limited examples of organic reactions is one of the problems of the amine–silanol paring system. To solve this problem, we investigated the use of silica–alumina as a more acidic support compared with silica for the preparation of acid–base bifunctional catalysts [13].

Silica–alumina-supported tertiary amine (SA-NEt_2) was prepared by the silane-coupling reaction between the silica–alumina surface and 3-(diethylamino) propyltrimethoxysilane in toluene solvent under reflux conditions (Scheme 1.8). The immobilization pathway of the silane-coupling reagents containing amine functional groups to silica–alumina surfaces was characterized by solid-state magic angle spinning nuclear magnetic resonance (MAS NMR) analysis. The silica–alumina was treated with a toluene solution of 3-(diethylamino)propyltrimethoxysilane for 5 min at room temperature, followed by filtration. The obtained solid was subjected to solid-state ^{13}C and ^{29}Si NMR analyses. It is well known that the ^{13}C NMR signal of the terminal carbon of the ethyl amino group shifts upfield by the interaction between acid (H^+) and the nitrogen atom. A ^{13}C NMR peak assignable to the terminal carbon of adsorbed

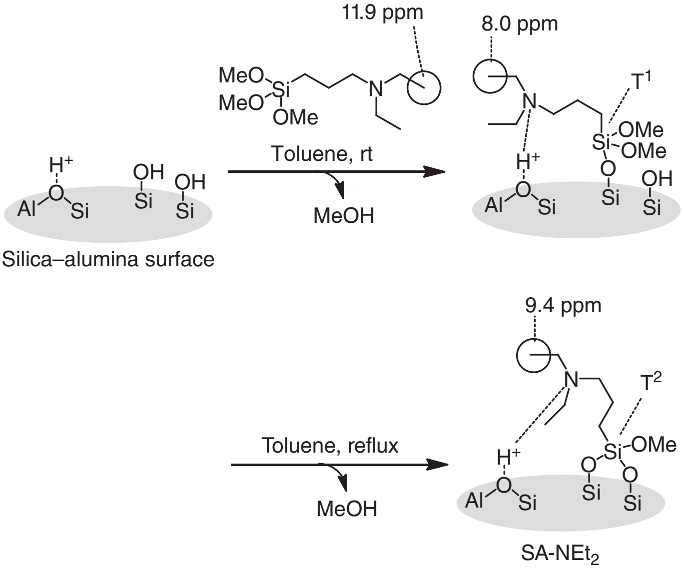

Scheme 1.8 Mechanism for tertiary amine immobilization on the SA surface.

amine group was observed around 8.0 ppm after the room-temperature treatment for 5 min, indicating that the acid–base interaction is stronger than that in SA-NEt$_2$ completely immobilized under reflux for 24 h (9.4 ppm) (Scheme 1.8). In ^{29}Si MAS NMR analysis, increasing T^2 site and decreasing T^1 site after the reflux were observed. From these results, the mechanism for the amine immobilization on the SA surface is proposed as follows (Scheme 1.8): (i) before the immobilization, the nitrogen atom of the tertiary amine interacts with the strong Brønsted acid site (Si-O(H$^+$)-Al) on the silica–alumina surface; (ii) one Si-OMe of the silane-coupling reagent reacts with surface Si-OH group near the strong acid site to form a covalent Si–O–Si(surface) bond; and (iii) another Si-OMe further reacts with neighboring Si-OH by heat treatment, thereby decreasing the acid–base interaction between the strong acid site and the nitrogen atom.

The signals of the mixtures of SA and triethylamine appeared at higher fields than of SA-NEt$_2$. For example, a peak of triethylamine adsorbed on the SA surface showed the largest upfield shift (11.8 (triethylamine in CDCl$_3$ solution) to 7.5 ppm). These results indicate that the acid–base interaction between the tertiary amine and the acid site on silica–alumina becomes weak by silane-coupling immobilization.

The Michael reaction of nitriles with unsaturated carbonyl compounds was examined using the SA-NEt$_2$ catalyst. As shown in Table 1.6, the SA-NEt$_2$ showed the highest catalytic activity for the Michael reaction of ethyl 2-cyanopropionate with ethyl acrylate to afford 2-cyano-2-methyl glutaric acid diethyl ester in 94% yield (entry 1). SiO$_2$-NEt$_2$ was much less active under the reaction conditions (entry 2). Neither triethylamine nor silica–alumina promoted the desired addition reaction (entries 3 and 4). Notably, the reaction scarcely proceeded with the

Table 1.6 Michael reactions with various catalysts.[a]

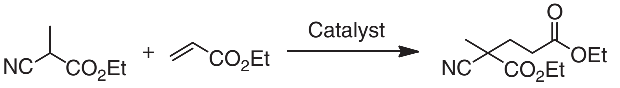

Entry	Catalyst	Yield (%)[b]
1	SA-NEt_2	94
2	SiO_2-NEt_2	9
3	Triethylamine	3
4[c]	Silica–alumina	1
5[c]	Triethylamine + silica–alumina	5

[a] Catalyst (0.09 mmol of amine), nitrile (1.0 mmol), ethyl acrylate (3 mmol), toluene (1 ml), 90 °C, 24 h, under N_2.
[b] Determined by GC and ^1H NMR. Based on the nitrile used.
[c] Silica–alumina (0.05 g).

mixture of triethylamine and silica–alumina (entry 5). Only in the case of the immobilized tertiary amine on the silica–alumina surface could the high catalytic performance be achieved. The high performance of SA-NEt_2 can be extended toward cyano-ethoxycarbonylation of various carbonyl compounds for the cyano-ethoxycarbonylation (Scheme 1.9).

Because of the weak interaction between the H^+ site and immobilized tertiary amine group, both the acid site and the amine group can act as catalytically active species. On the other hand, a nonimmobilized tertiary amine, such as triethylamine, strongly adsorbed on the acid site and deactivated each other. Therefore, SA-NEt_2 showed much higher activity for the above-mentioned Michael reaction and cyano-ethoxycarbonylation. These reactions hardly occurred with only silica–alumina or the tertiary amine. The catalytic reaction pathway including acid–base cooperative activation is shown in Scheme 1.10. Similar to the case of silica–alumina, Al-MCM-41 was also reported as a support, which can enhance the amine-catalyzed nitroaldol reaction [14].

1.3.3
Control of Acid–Base Interaction on Solid Surface

To more precisely control the acid–base interaction of the silica–alumina-supported tertiary amine catalyst for organic synthesis, we examined the control of the density of surface Si-OH groups [15]. According to the above-mentioned immobilization mechanism, if the Si-OH density decreases, the acid–base interaction should be decease because of the far amine-immobilization positions from strong acid sites, resulting in lower acid–base interaction and higher catalytic performance.

Silica–alumina was pretreated at 120–500 °C under vacuum before using it as a support for amines. The treated samples are denoted as SA (treatment temperature, *T*). Tertiary amines were immobilized on the SA(*T*) by treating

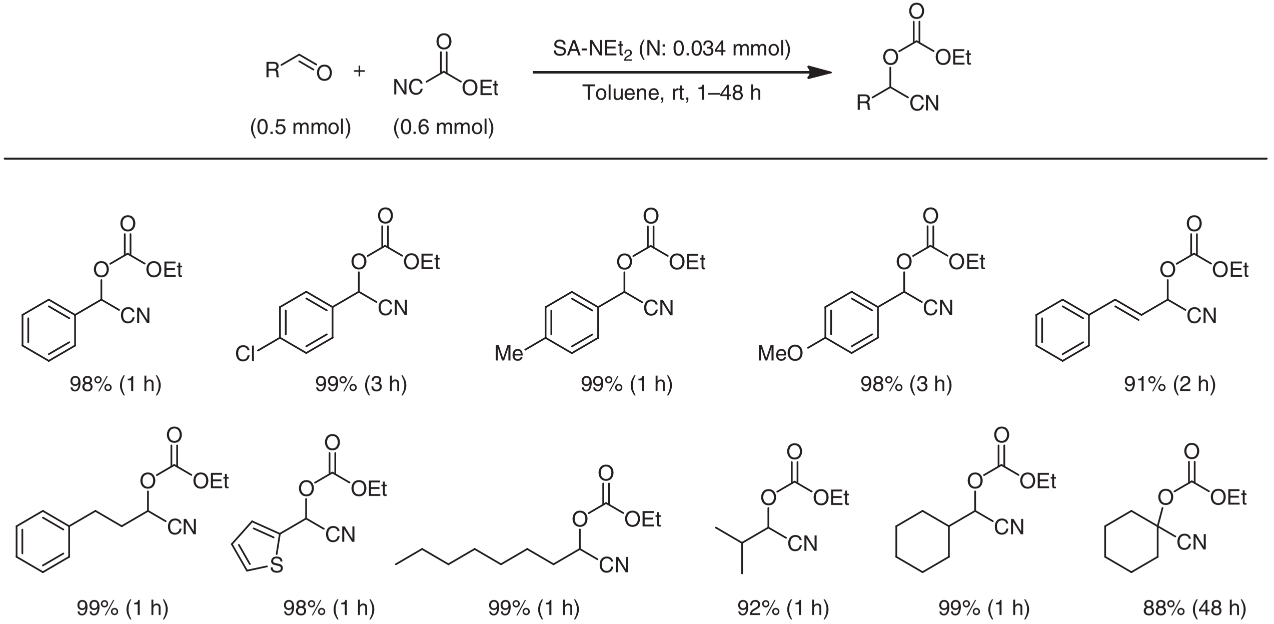

Scheme 1.9 Cyano-ethoxycarbonylation of various carbonyl compounds using the silica–alumina-supported tertiary amine catalyst (SA-NEt_2).

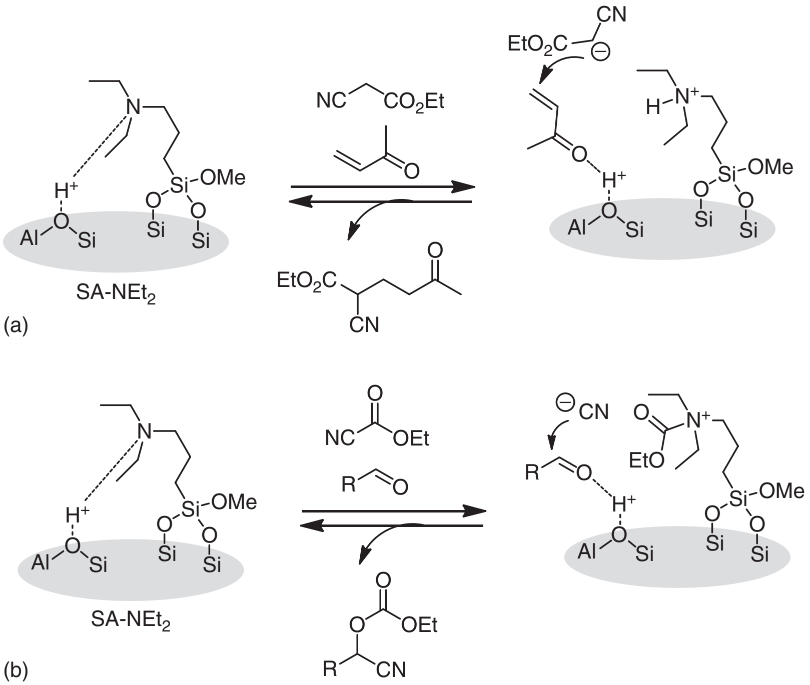

Scheme 1.10 Reaction pathways of SA-NEt$_2$-catalyzed (a) Michael reaction and (b) cyano-ethoxycarbonylation.

the latter with a toluene solution of 3-(diethylamino)propyltrimethoxysilane under reflux for 24 h. Scheme 1.11 represents the preparation pathway of SA(500)-NEt$_2$. ^{13}C MAS NMR analysis was conducted to determine the acid–base interaction between the strong acid site and the immobilized amine group. As above, after the immobilization of tertiary amine groups onto SA(120), the ^{13}C NMR signal of the terminal carbon (9.4 ppm) shifted upfield compared to that of the amine precursor (11.9 ppm) (Scheme 1.8). On the other hand, a signal for the SA(500)-NEt$_2$ was observed at 11.0 ppm (Scheme 1.11), which showed only a very small shift from the precursor. Additionally, contact-time array ^{13}C CP/MAS NMR (CP, cross polarization) measurements of SA(500)-NEt$_2$ and SA(120)-NEt$_2$ were conducted to determine the molecular mobility of immobilized amines. This variable-contact-time ^{13}C CP/MAS NMR is a technique to determine the molecular motion of solid materials [16]. As CP is a measure of the efficiency of magnetization transfer by the dipolar coupling from ^{1}H to ^{13}C, it is most efficient for the static ^{1}H–^{13}C dipolar interactions. As a result, the less mobile carbon groups exhibit a higher CP rate, and the NMR signal intensity becomes stronger with a relatively short CP contact time. This signal becomes weak with prolonged contact time because of the attenuation of the transferred magnetization. On the other hand, the signal intensity of a molecule with high mobility shows strong intensity with relatively long contact time [16]. Figure 1.5 shows the normalized intensity of ^{13}C CP/MAS

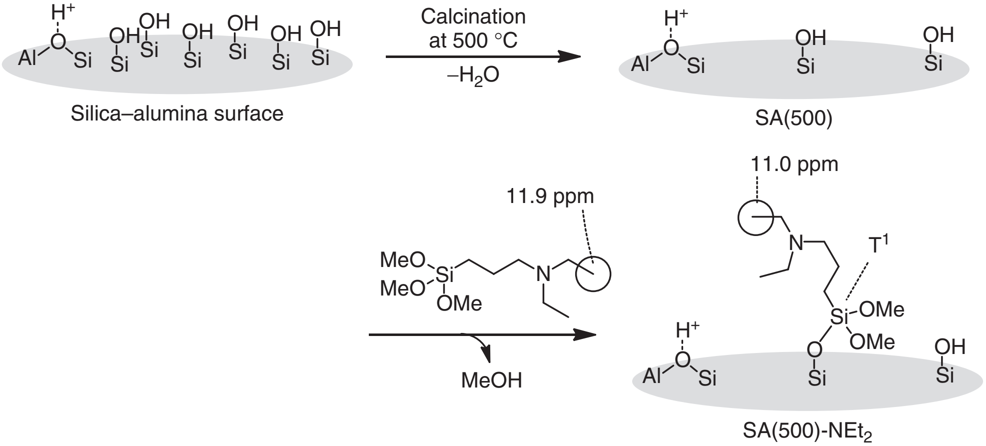

Scheme 1.11 Preparation step for SA(500)-NEt$_2$.

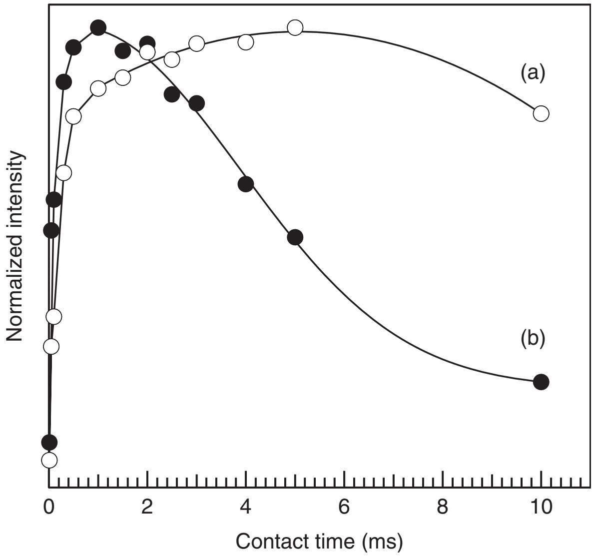

Figure 1.5 Dependence of the normalized intensity of variable-contact-time ^{13}C CP/MAS NMR spectra for the terminal carbon on contact time: (a) SA(500)–NEt$_2$ (○) and (b) SA(120)–NEt$_2$ (•).

NMR spectra for amine terminal carbon (9–11 ppm) versus contact time curves on SA(500)-NEt$_2$ and SA(120)-NEt$_2$. Variable-contact-time data on SA(500)-NEt$_2$ showed the highest intensity of terminal carbon with 5.0 ms contact time. In contrast, the highest intensity on SA(120)-NEt$_2$ was at 1.0 ms contact time. Thus, the CP time constant (T_{CH}) values of SA(500)-NEt$_2$ are much longer than those of the SA(120)-NEt$_2$, indicating the much higher mobility of the tertiary amine group in SA(500)-NEt_2. The strong acid–base interaction between the amine group and acid site on the silica–alumina in SA(120)-NEt_2 suppressed the tertiary amine mobility compared with SA(500)-NEt_2. The calcination of SA at 500 °C reduced the amount of surface silanol groups, resulting in high dispersion of silanols on the SA surface, and as a result the amine might be immobilized at a position far away from a strong acid site (Scheme 1.11). On the other hand, in the case of a SA(120) support with the higher concentration of Si-OH groups, the amine group–acid site distance can become closer compared to that on SA(500) (Scheme 1.8), suggesting strong acid–base interaction.

The 1,4-addition reaction of nitroethane to methyl vinyl ketone was examined using SA(*T*)-NEt_2. Results are summarized in Table 1.7. The catalyst

Table 1.7 1,4-Addition of nitroethane to methyl vinyl ketone by various catalysts.[a]

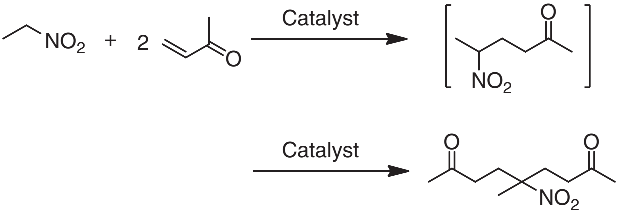

Entry	Catalyst	Conversion of nitroethane (%)[b]	Yield of dialkylated product (%)[b]	Initial rate (mmol h^{-1})[b,c]
1[d]	SA(500)-NEt_2	99	93	0.53
2	SA(500)-NEt_2	99	86	0.53
3	SA(400)-NEt_2	99	82	0.41
4	SA(200)-NEt_2	99	80	0.36
5	SA(120)-NEt_2	99	74	0.28
6	SiO_2(120)-NEt_2	84	49	0.16
7	SiO_2(500)-NEt_2	76	14	0.13
8[e]	SA(500)	22	0	0.02
9	NEt_3	16	2	<0.01
10[e]	SA(500) + NEt_3	99	28	0.27
11	NaOEt	99	1[f]	n.d.
12	None	0	0	—

[a] Reaction conditions: nitroethane (1 mmol), methyl vinyl ketone (3 mmol), catalyst (amine: 4.5×10^{-2} mmol), toluene (1 ml), 50 °C, 20 h, under N_2.

[b] Determined by ^{1}H NMR and GC using internal standard technique. Based on nitroethane used. Other byproducts were not detected except for mono-alkylated product in the case of supported catalysts.

[c] Initial formation rate of the addition products.

[d] 24 h.

[e] 0.08 g of SA was used.

[f] A byproduct was formed by cyclization reaction.

SA(500)-NEt_2 was found to be remarkably active to afford the double alkylated product in 93% yield (entry 1). Decreasing the pretreatment temperature of silica–alumina reduced the catalytic activity of SA(T)-NEt_2 (entries 1–4). It is to be noted that this reaction scarcely proceeded with either SA(500) or homogeneous amines (entries 8 and 9). A mixture of SA(500) and triethylamine showed a catalytic activity, but the yield of the product was very low (entry 10). It is indicated that both the surface acid site and the amine group in SA(500)-NEt_2 without acid–base neutralization act as catalytically active species. The reaction pathway might be similar to the case of 1,4-addition of nitriles (Scheme 1.10a).

In the case of a strong base, such as sodium ethoxide, as a homogeneous catalyst, the selectivity was as low as 1–7% during the whole course of the reaction due to further conversion of the product toward an undesired cyclization product (entry 11) [17]. The cooperative activation by the surface acid and amine group, which is a weaker base compared to sodium ethoxide, realizes selective catalysis compared to when using only a strong base.

1.3.4
Cooperative Catalysis of Acid Site, Primary Amine, and Tertiary Amine

We also disclosed a cooperative catalysis of both primary and tertiary amine-immobilized silica–alumina surface (SA-NH_2-NEt_2) [18]. The surface structure of the catalyst is shown in Figure 1.6. The activity of the trifunctional catalyst for the nitroaldol reaction is much higher than that for the only primary or tertiary amine immobilized silica–alumina, as shown in Table 1.8. The catalysis of the double-amine-immobilized silica–alumina is highlighted by the reaction using an acidic functional group. It should be noted that benzaldehyde with a carboxyl group also reacted with nitromethane in the presence of the SA-NH_2-NEt_2 catalyst, affording 65% yield of the corresponding 1,3-dinitroalkane product (Scheme 1.12). This reaction scarcely proceeded with sodium methoxide as a strong base because of neutralization of the base with the carboxylic acid.

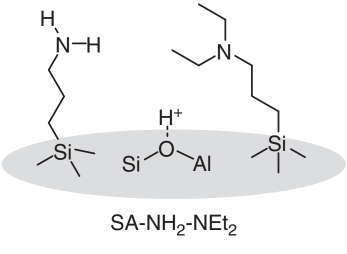

Figure 1.6 Surface structure of SA-NH_2-NEt_2.

Table 1.8 Nitroaldol reactions of nitromethane with benzaldehyde using various catalysts.[a]

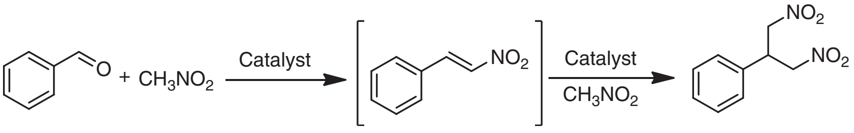

Entry	Catalyst	Conversion rate of benzaldehyde (mmol h^{-1})[b]
1	SA-NH_2-NEt_2	1.87
2	SA-NH_2 + SA-NEt_2	0.13
3	SA-NH_2	0.03
4	SA-NEt_2	0.08
5[c]	Silica–alumina + *n*-hexylamine + triethylamine	0.31
6	*n*-Hexylamine + triethylamine	0.26
7[c]	Silica–alumina	<0.01

[a] Reaction conditions: benzaldehyde (5 mmol), nitromethane (2 ml), catalyst (NH_2: 0.015 mmol, NEt_2: 0.012 mmol), 100 °C, under N_2.
[b] Determined by GC and ^{1}H NMR.
[c] Silica–alumina (0.034 g).

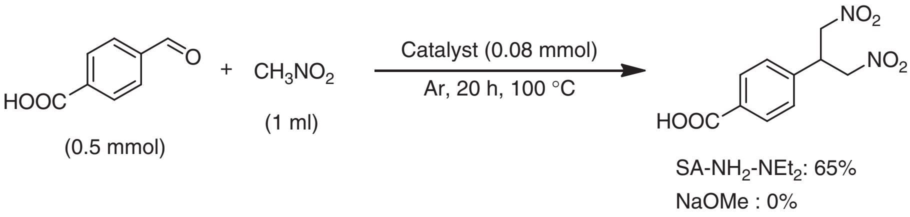

Scheme 1.12 Reaction of *p*-formylbenzoic acid with nitromethane.

1.4
Prospect

Acid–base cooperative catalysis by organofunctionalized solid surfaces was summarized in this chapter. While several bifunctional silica catalysts having both organic acid and base groups have been reported, their real catalytic activities strongly depend on the density and arrangement of silanol groups on silica surfaces. Strong OH H^+ acid sites of silica–alumina surfaces can also act as active sites for the cooperative catalysis with immobilized amines, which realizes various organic transformations. More precisely controlled synthesis of catalyst surfaces involving acid and base sites is needed for the higher class of research. Utilization of metal functions by immobilization of metal complexes and clusters is also desired for further extensions and more applications of cooperative catalysis to a variety of organic syntheses at solid surfaces.

References

1. For reviews, see: (a) Gröger, H. (2001) *Chem. Eur. J.*, **7**, 5246. (b) Kanai, M., Kato, N., Ichikawa, E., and Shibasaki, M. (2005) *Pure Appl. Chem.*, **77**, 2047. See also: (c) Shen, Y., Feng, X., Li, Y., Zhang, G., and Jiang, Y. (2003) *Tetrahedron*, **59**, 5667. (d) Kanemasa, S. and Ito, K. (2004) *Eur. J. Org. Chem.*, 4741. (e) Ma, J.-A. and Cahard, D. (2004) *Angew. Chem. Int. Ed.*, **43**, 4556. (f) Wang, Y., Li, H., Wang, Y.-Q., Liu, Y., Foxman, B.M., and Deng, L. (2007) *J. Am. Chem. Soc.*, **129**, 6364. (g) Lin, Y.-M., Boucau, J., Li, Z., Casarotto, V., Lin, J., Nguyen, A.N., and Ehrmantraut, J. (2007) *Org. Lett.*, **9**, 567. (h) Tsogoeva, S.B., Hateley, M.J., Yalalov, D.A., Meindl, K., Weckbecker, C., and Huthmacher, K. (2005) *Bioorg. Med. Chem.*, **13**, 5680.
2. (a) Voit, B. (2006) *Angew. Chem. Int. Ed.*, **45**, 4238. (b) Gelman, F., Blum, J., and Avnir, D. (2001) *Angew. Chem. Int. Ed.*, **40**, 3647. (c) Motokura, K., Fujita, N., Mori, K., Mizugaki, T., Ebitani, K., and Kaneda, K. (2005) *J. Am. Chem. Soc.*, **127**, 9674. (d) Helms, B., Guillaudeu, S.J., Xie, Y., McMurdo, M., Hawker, C.J., and Fréchet, J.M.J. (2005) *Angew. Chem. Int. Ed.*, **44**, 6384. (e) Phan, N.T.S., Gill, C.S., Nguyen, J.V., Zhang, Z.J., and Jones, C.W. (2006) *Angew. Chem. Int. Ed.*, **45**, 2209. (f) Pilling, A.W., Boehmer, J., and Dixon, D.J. (2007) *Angew. Chem. Int. Ed.*, **46**, 5428. (g) Motokura, K., Tada, M., and Iwasawa, Y. (2009) *J. Am. Chem. Soc.*, **131**, 7944.
3. (a) Margelefsky, E.L., Zeidan, R.K., and Davis, M.E. (2008) *Chem. Soc. Rev.*, **37**, 1118. (b) Motokura, K., Tada, M., and Iwasawa, Y. (2008) *Chem. Asia J.*, **3**, 1230. (c) Shylesh, S. and Thiel, W.R. (2011) *ChemCatChem*, **3**, 278.
4. Huh, S., Chen, H.-T., Wiench, J.W., Pruski, M., and Lin, V.S.-Y. (2005) *Angew. Chem. Int. Ed.*, **44**, 1826.
5. (a) Zeidan, R.K., Hwang, S.-J., and Davis, M.E. (2006) *Angew. Chem. Int. Ed.*, **45**, 6332. (b) Zeidan, R.K. and Davis, M.E. (2007) *J. Catal.*, **247**, 379.
6. (a) Shylesh, S., Wagner, A., Seifert, A., Ernst, S., and Thiel, W.R. (2009) *Chem. Eur. J.*, **15**, 7052. (b) Shang, F., Sun, J., Wu, S., Liu, H., Guan, J., and Kan, Q. (2011) *J. Colloid Interface Sci.*, **355**, 190.
7. Brunelli, N.A., Venkatasubbaiah, K., and Jones, C.W. (2012) *Chem. Mater.*, **24**, 2433.
8. Kubota, Y., Goto, K., Miyata, S., Goto, Y., Fukushima, Y., and Sugi, Y. (2003) *Chem. Lett.*, **32**, 234.
9. Bass, J.D., Solovyov, A., Pascall, A.J., and Katz, A. (2006) *J. Am. Chem. Soc.*, **128**, 3737.
10. Sharma, K.K. and Asefa, T. (2007) *Angew. Chem. Int. Ed.*, **119**, 2937.
11. Takahashi, T., Watahiki, T., Kitazume, S., Yasuda, H., and Sakakura, T. (2006) *Chem. Commun.*, 1664.
12. Motokura, K., Itagaki, S., Iwasawa, Y., Miyaji, A., and Baba, T. (2009) *Green Chem.*, **11**, 1876.
13. (a) Motokura, K., Tada, M., and Iwasawa, Y. (2007) *J. Am. Chem. Soc.*, **129**, 9540. (b) Motokura, K., Tomita, M., Tada, M., and Iwasawa, Y. (2008) *Chem. Eur. J.*, **14**, 4017.
14. Shylesh, S., Wagener, A., Seifert, A., Ernst, S., and Thiel, W.R. (2010) *ChemCatChem*, **2**, 1231.
15. Motokura, K., Tanaka, S., Tada, M., and Iwasawa, Y. (2009) *Chem. Eur. J.*, **15**, 10871.
16. (a) Wang, L.-Q., Liu, J., Exarhos, G.J., Flanigan, K.Y., and Bordia, R. (2000) *J. Phys. Chem. B*, **104**, 2810. (b) Sahoo, S.K., Kim, D.W., Kumar, J., Blumstein, A., and Cholli, A.L. (2003) *Macromolecules*, **36**, 2777. (c) Kao, H.-M., Hung, T.-T., and Fey, G.T.K. (2007) *Macromolecule*, **40**, 8673.
17. (a) Wada, M., Tsuboim, A., Nishimura, K., and Erabi, T. (1987) *Nippon Kagaku Kaishi*, **7**, 1284. (b) Berrocal, M.V., Gil, M.V., Roman, E., Serrano, J.A., Hursthouse, M.B., and Light, M.E. (2005) *Tetrahedron Lett.*, **46**, 3673.
18. Motokura, K., Tada, M., and Iwasawa, Y. (2008) *Angew. Chem. Int. Ed.*, **47**, 9230.